

Doubly Fed Induction Generator for Wind Energy Conversion Systems with Integrated Active Filter Capabilities

PotuVineetha

B.Tech Student,

**Mahatma Gandhi Institute of Technology,
Hyderabad.**

Bhashabolna Rajesh Varma

B.Tech Student,

**Scient Institute of Engineering & Technology
Hyderabad.**

Abstract:

Doubly Fed Induction Generator for Wind Energy Conversion Systems deals with the operation of doubly fed induction generator (DFIG) with an integrated active filter capabilities using grid-side converter (GSC). The main contribution of this work lies in the control of GSC for supplying harmonics in addition to its slip power transfer. The rotor-side converter (RSC) is used for attaining maximum power extraction and to supply required reactive power to DFIG. Wind energy conversion system (WECS) works as a static compensator (STATCOM) for supplying harmonics even when the wind turbine is in shutdown condition. Control algorithms of both GSC and RSC are presented in detail. Implemented project DFIG-based WECS is simulated using MATLAB/Simulink. A prototype of the proposed DFIG based WECS is developed using a digital signal processor (DSP). The wind energy is the preferred for all renewable energy sources. In the initial days, wind turbines have been used as fixed speed wind turbines with squirrel cage induction generator and capacitor banks. Most of the wind turbines are fixed speed because of their simplicity and low cost.

PROSED SYSTEM:

- Operation of doubly fed induction generator (DFIG) with an integrated active filter capabilities using grid-side converter (GSC).
- The control of GSC for supplying harmonics in addition to its slip power transfer.

- The rotor-side converter (RSC) attaining maximum power extraction.
- This wind energy conversion system (WECS) works as a static compensator (STATCOM) for supplying harmonics (even when the wind turbine is in shutdown condition).
- Control algorithms of both GSC and RSC are implemented

TECHNOLOGY:

- DFIG(doubly fed induction generator)
- GSC(grid-side converter)
- RSC(rotor-side converter)
- WECS (wind energy conversion system)
- STATCOM (static compensator)
- UPQC (A super capacitor energy storage system at the dc link of unified power quality conditioner.)

Future scope:

The increase in population and industrialization, the energy demand has increased significantly. The conventional energy sources such as coal, oil, and gas are limited in nature. There is a need for renewable energy sources for the future energy demand. The other main advantages of this renewable source are eco-friendliness and unlimited in nature. Due to technical advancements, the cost of the wind power produced is comparable to that of conventional power plants. Therefore, the wind energy is the most preferred out of all renewable energy sources. In the initial days, wind turbines have been used as fixed speed wind turbines with squirrel cage induction

generator and capacitor banks. Most of the wind turbines are fixed speed because of their simplicity and low cost. By observing and implementing wind turbine characteristics, one can clearly identify that for extracting maximum power, the machine should run at varying rotor speeds at different wind speeds. An implemented modern power electronic converter, the machine is able to run at adjustable speeds. These variable speed wind turbines are able to improve the wind energy production. Out of all variable speed wind turbines, doubly fed induction generators (DFIGs) are preferred because of their low cost. The advantages of this DFIG are the higher energy output, lower converter rating, and better utilization of generators.

INTRODUCTION:

These DFIGs also provide good damping performance for the weak grid. Independent control of active and reactive power is achieved by the decoupled vector control algorithm. This vector control of such system is usually realized in synchronously rotating reference frame oriented in either voltage axis or flux axis. In this work, the control of rotor-side converter (RSC) is implemented in voltage-oriented reference frame. Response of DFIG-based wind energy conversion system (WECS) to grid disturbance is compared to the fixed speed WECS. Generated power smoothening is achieved by implementing super magnetic energy storage systems.

The other auxiliary services such as reactive power requirement and transient stability limit are achieved by including static compensator (STATCOM). A distribution STATCOM (DSTATCOM) coupled with fly-wheel energy storage system is used at the wind farm for mitigating harmonics and frequency disturbances. A super capacitor energy storage system at the dc link of unified power quality conditioner (UPQC) improving power quality and reliability. The harmonics compensation and reactive power control are achieved with the help of existing RSC. An indirect current control technique is simple and shows better performance for eliminating harmonics as compared to direct current control.

The Harmonics are injected from the RSC into the rotor windings. This creates losses and noise in the machine.

Working principle:

In this work, a new control algorithm for GSC is proposed for compensating harmonics produced by nonlinear loads using an indirect current control. RSC is used for controlling the reactive power of DFIG. The other main advantage of proposed DFIG is that it works as an active filter even when the wind turbine is in shutdown condition. Therefore, it compensates load reactive power and harmonics at wind turbine stalling case. Both simulation and experimental performances of the proposed integrated active filter-based DFIG are presented in this work. The dynamic performance of the proposed DFIG is also demonstrated for varying wind speeds and changes in unbalanced nonlinear loads at point of common coupling (PCC).

Configuration of System and Operating Principle:

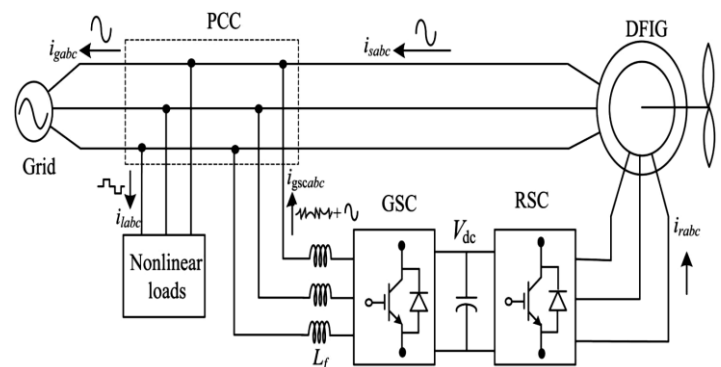


Fig. 1. Proposed system configuration

Above figure shows a schematic diagram of the proposed DFIGbased WECS with integrated active filter capabilities. DFIG, the stator is directly connected to the grid as shown in Fig. 1. Two back-to-back connected voltage source converters (VSCs) are placed between the rotor and the grid. Nonlinear loads are connected at PCC as shown in Fig. 1. The proposed DFIG works as an active filter in addition to the active power generation similar to normal DFIG. Harmonics generated by the nonlinear load connected at the PCC distort the PCC voltage.

RSC is controlled for achieving maximum power point tracking (MPPT) and also for making unity power factor at the stator side using voltage-oriented reference frame. Synchronous reference frame (SRF) control method is used for extracting the fundamental component of load currents for the GSC control.

DESIGN OF DFIG-BASED WECS:

Selection of ratings of VSCs and dc-link voltage is very much important for the successful operation of WECS.

Selection of DC-Link Voltage:

The dc-link voltage of VSC must be greater than twice the peak of maximum phase voltage. While considering from the rotor side, the rotor voltage is slip times the stator voltage. So, the design criteria for the selection of dc-link voltage can be achieved by considering only PCC voltage. While considering from the GSC side, the PCC line voltage (V_{ab}) is 230 V, as the machine is connected in delta mode.

Therefore, the dc-link voltage is estimated as

$$V_{dc} \geq \frac{2\sqrt{2}}{\sqrt{3} * m} V_{ab}$$

where

- V_{ab} is the line voltage at the PCC.
- Maximum modulation index is selected as 1 for linear range.
- The value of dc-link voltage (V_{dc}) by (1) is estimated as 375 V.
- Hence, it is selected as 375 V.

Selection of VSC Rating

The DFIG draws a lagging volt-ampere reactive (VAR) for its excitation to build the rated air gap voltage. , the rating of the VSC used as RSC S_{rated} is given as

$$S_{rated} = \sqrt{P_{r,max}^2 + Q_{r,max}^2}$$

Design of Interfacing Inductor.

The design of interfacing inductors between GSC and PCC depends upon allowable GSC current limit (i_{gscpp}), dc-link voltage, and switching frequency of GSC. Maximum possible GSC line currents are used for the calculation. Maximum line current depends upon the maximum power and the line voltage at GSC. The maximum possible power in the GSC is the slip power. Interfacing inductor between PCC and GSC is selected as 4 mH.

$$L_i = \frac{\sqrt{3} m v_{dc}}{12 a f_m \Delta i_{gsc}}$$

$$= \frac{\sqrt{3} \times 1 \times 375}{12 \times 1.5 \times 10\,000 \times 0.25 \times 3.76} = 3.8 \text{ mH.}$$

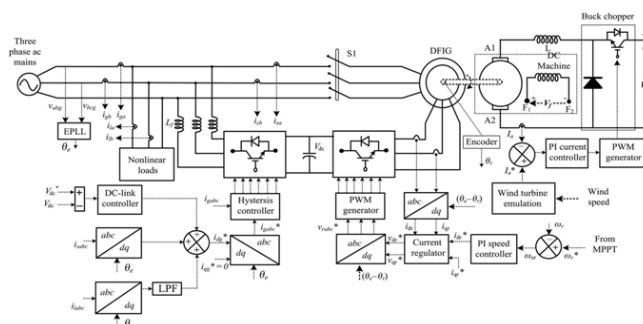


Fig. 2. Control algorithm of the proposed WECS.

CONTROL STRATEGY:

Control algorithms for both GSC and RSC are presented in this section. The control algorithm for emulating wind turbine characteristics using dc machine and Type A chopper is also shown in Fig. 2.

Control of RSC:

The main purpose of RSC is to extract maximum power with independent control of active and reactive powers. Here, the RSC is controlled in voltage-oriented reference frame., the active and reactive powers are controlled by controlling direct and quadrature axis rotor currents (i_{dr} and i_{qr})

$$i_{dr}^*(k) = i_{dr}^*(k-1) + k_{pd} \{ \omega_{er}(k) - \omega_{er}(k-1) \} + k_{id} \omega_{er}(k)$$

Where:

- The speed error (ω_e) is obtained by subtracting sensed speed (ω_r) from the reference speed (ω^*r).
- k_{pd} and k_{id} are the proportional and integral constants of the speed controller.
- $\omega_e(k)$ and $\omega_e(k-1)$ are the speed errors at k th and $(k-1)$ th instants.
- $i^*_{dr}(k)$ and $i^*_{dr}(k-1)$ are the direct axis rotor reference current at k th and $(k-1)$ th instants.
- Reference rotor speed (ω^*r).

In general, the quadrature axis reference rotor current (i^*_{qr}) is selected such that the stator reactive power (Q_s) is made zero. In this DFIG, quadrature axis reference rotor current (i^*_{qr}) is selected for injecting the required reactive power. Inner current control loops are taken for control of actual direct and quadrature axis rotor currents (i_{dr} and i_{qr}) close to the direct and quadrature axis reference rotor currents (i^*_{dr} and i^*_{qr}). The rotor currents i_{dr} and i_{qr} are calculated from the sensed rotor currents (i_{ra} , i_{rb} , and i_{rc}).

$$i_{dr} = \frac{2}{3} \begin{bmatrix} i_{ra} \sin \theta_{slip} + i_{rb} \sin (\theta_{slip} - 2\pi/3) \\ + i_{rc} \sin (\theta_{slip} + 2\pi/3) \end{bmatrix}$$

$$i_{qr} = \frac{2}{3} \begin{bmatrix} i_{ra} \cos \theta_{slip} + i_{rb} \cos (\theta_{slip} - 2\pi/3) \\ + i_{rc} \cos (\theta_{slip} + 2\pi/3) \end{bmatrix}$$

$$\theta_{slip} = \theta_e - \theta_r$$

where θ_e is calculated from PLL for aligning rotor currents into voltage axis. The rotor position (θ_r) is achieved with an encoder. Direct and quadrature axis rotor voltages (v_{dr} and v_{qr}) are obtained from direct and quadrature axis rotor current errors (i_{der} and i_{qer}) as

$$v'_{dr}(k) = v'_{dr}(k-1) + k_{pdv} \{i_{der}(k) - i_{der}(k-1)\} + k_{idv} i_{der}(k)$$

$$v'_{qr}(k) = v'_{qr}(k-1) + k_{pqv} \{i_{qer}(k) - i_{qer}(k-1)\} + k_{iqv} i_{qer}(k)$$

Where:

$$i_{der} = i^*_{dr} - i_{dr} \quad \text{and} \quad i_{qer} = i^*_{qr} - i_{qr}$$

Where:

k_{pdv} and k_{idv} are the proportional and integral gains of direct axis current controller. k_{pqv} and k_{iqv} are the proportional and integral gains of quadrature axis current controller. Direct and quadrature components are decoupled by adding some compensating terms as

$$v^*_{dr} = v'_{dr} + (\omega_e - \omega_r) \sigma L_r i_{qr}$$

$$v^*_{qr} = v'_{qr} - (\omega_e - \omega_r) (L_m i_{ms} + \sigma L_r i_{dr}).$$

These reference direct and quadrature voltages (v^*_{dr} , v^*_{qr}) are converted into three phase reference rotor voltages (v^*_{ra} , v^*_{rb} , v^*_{rc}) as

$$v^*_{ra} = v^*_{dr} \sin \theta_{slip} + v^*_{qr} \cos \theta_{slip}$$

$$v^*_{rb} = v^*_{dr} \sin (\theta_{slip} - 2\pi/3) + v^*_{qr} \cos (\theta_{slip} - 2\pi/3)$$

$$v^*_{rc} = v^*_{dr} \sin (\theta_{slip} + 2\pi/3) + v^*_{qr} \cos (\theta_{slip} + 2\pi/3).$$

These three phase rotor reference voltages (v^*_{ra} , v^*_{rb} , v^*_{rc}) are compared with triangular carrier wave of fixed switching frequency for generating pulse-width modulation (PWM) signals for the RSC.

Control of GSC:

The novelty of this work lies in the control of this GSC for mitigating the harmonics produced by the nonlinear loads. The control block diagram of GSC is shown in Fig. 2. Here, an indirect current control is applied on the grid currents for making them sinusoidal and balanced. Therefore, this GSC supplies the harmonics for making grid currents sinusoidal and balanced. These grid currents are calculated by subtracting the load currents from the summation of stator currents and GSC currents. Active power component of GSC current is obtained by processing the dc-link voltage error (v_{dce}) between reference and estimated dc-link voltage (V^*_{dc} and V_{dc}) through PI controller as

$$i_{gsc}^*(k) = i_{gsc}^*(k-1) + k_{pdc} \{v_{dce}(k) - v_{dce}(k-1)\} + k_{idc} v_{dce}(k)$$

Where k_{pdc} and k_{idc} are proportional and integral gains of dc-link voltage controller. $V_{dce}(k)$ and $V_{dce}(k-1)$ are dclink voltage errors at k th and $(k-1)$ th instants. $i_{*gsc}(k)$ and $i_{*gsc}(k-1)$ are active power component of GSC current at k th and $(k-1)$ th instants. Active power component of stator current (i_{ds}) is obtained from the sensed stator currents (i_{sa} , i_{sb} , and i_{sc}) using abc to dq transformation as

$$i_{ds} = 2/3 [i_{sa} \sin \theta_e + i_{sb} \sin(\theta_e - 2\pi/3) + i_{sc} \sin(\theta_e + 2\pi/3)].$$

Fundamental active load current (i_{ld}) is obtained using SRF theory [33]. Instantaneous load currents (i_{labc}) and the value of phase angle from EPLL are used for converting the load currents in to synchronously rotating dq frame (i_{ld}). In synchronously rotating frames, fundamental frequency currents are converted into dc quantities and all other harmonics are converted into non-dc quantities with a frequency shift of 50 Hz. DC values of load currents in synchronously rotating dq frame (i_{ld}) are extracted using low-pass filter (LPF). Direct axis component of reference grid current (i_{*gd}) is obtained from the direct axis current of stator current (i_{ds}) and load current (i_{ld}) in synchronously rotating frame and the loss component of GSC current (i_{*gsc}) as

$$i_{*gd} = i_{*gsc} + i_{ds} - \overline{i_{ld}}.$$

Quadrature axis component of reference grid current (i_{*gq}) is selected as zero for not to draw any reactive power from grid. Reference grid currents (i_{*ga} , i_{*gb} , and i_{*gc}) are calculated from the direct and quadrature axis grid currents (i_{*gd} , i_{*gq}). The hysteresis current controller is used to generate switching pulses for the GSC. The hysteresis controller is a feedback current control where sensed current tracks the reference current within a hysteresis band (i_{hb}).

At every sampling instant, the actual current (i_{gabc}) is compared to the reference current (i_{*gabc}) as

$$\Delta i_{gabc} = i_{*gabc} - i_{gabc}$$

When $\Delta i_{gabc} > i_{hb}$, lower switch is turned ON.

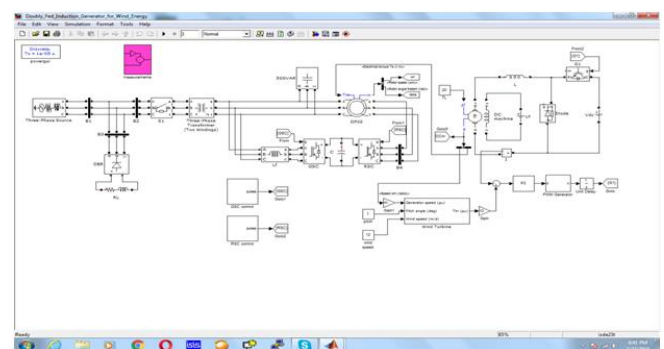
When $\Delta i_{gabc} < -i_{hb}$, upper switch is turned ON.

Using these equations, gating pulses for three phases of GSC are generated in the same way.

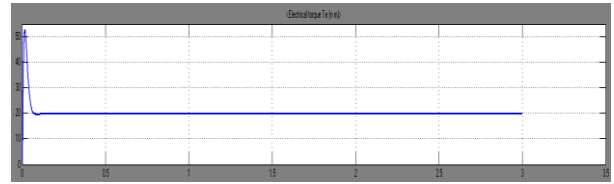
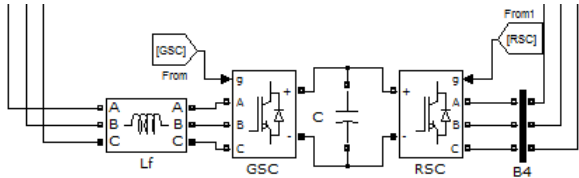
CONCLUSION:

GSC control algorithm of the implemented DFIG has been modified for supplying the harmonics and reactive power of the loads. Proposed DFIG, the reactive power for the induction machine has been supplied from the RSC and the load reactive power has been supplied from the GSC. Decoupled control of both active and reactive powers has achieved by RSC control. DFIG has also been verified at wind turbine stalling condition for compensating harmonics and reactive power of local loads. Proposed DFIG-based WECS with an integrated active filter has been simulated using MATLAB/Simulink environment, and the simulated results are verified with test results of the developed prototype of this WECS. Steady-state performance of the proposed DFIG has been demonstrated for a wind speed. Dynamic performance of this proposed GSC control algorithm has also been verified for the variation in the wind speeds and for local nonlinear load.

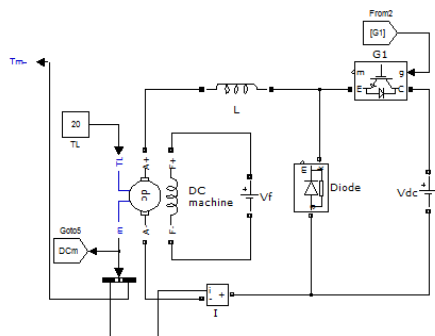
Experimental Result



Simulation in Matlab

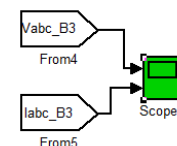
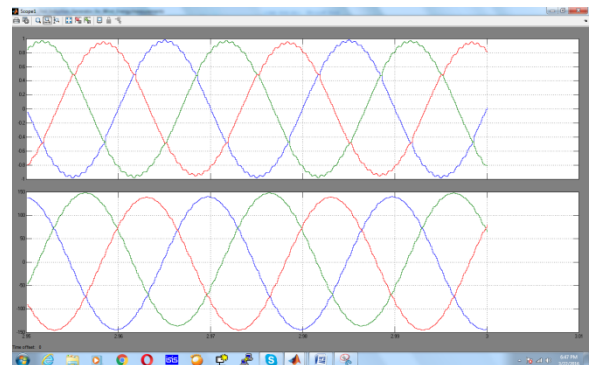
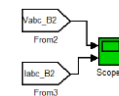
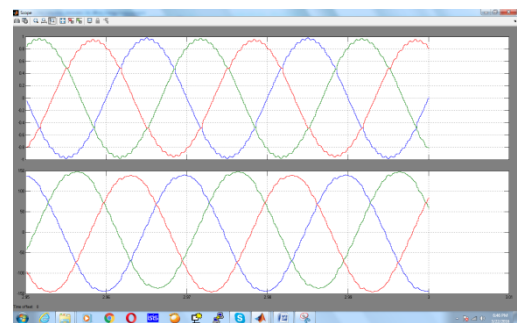
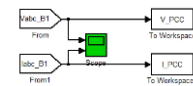
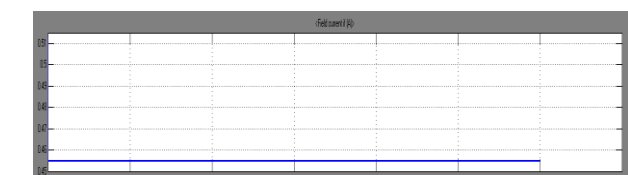
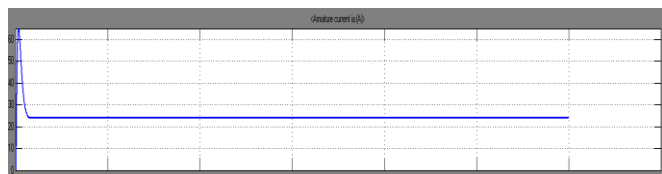
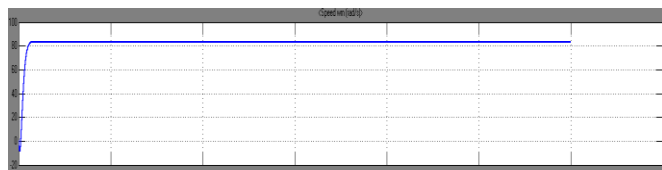
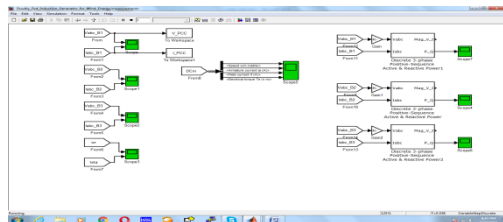


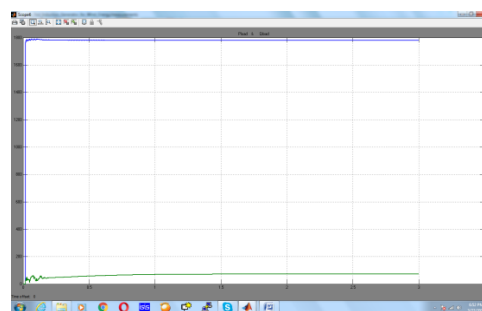
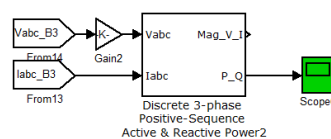
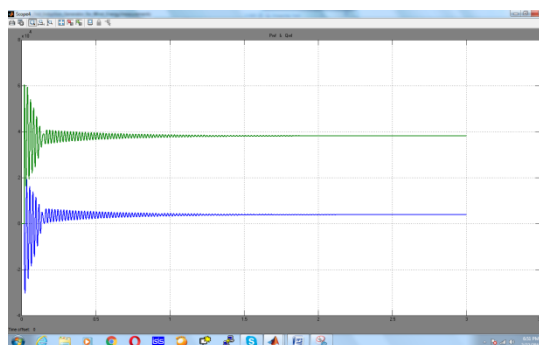
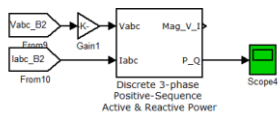
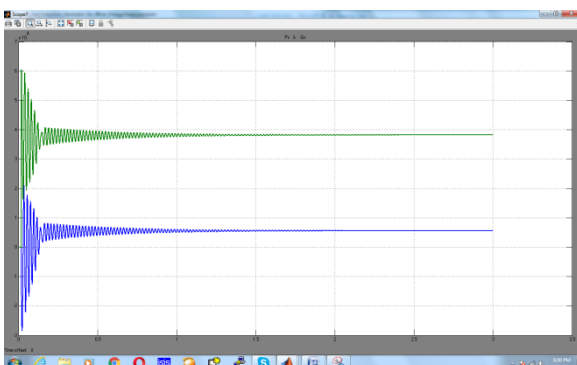
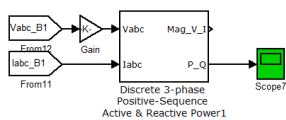
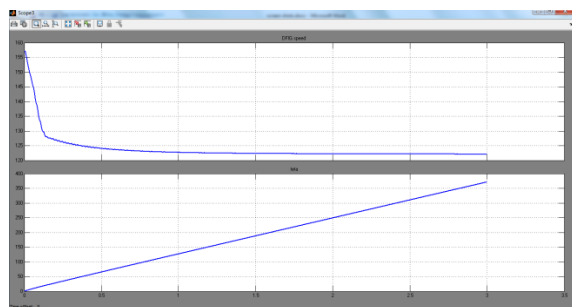
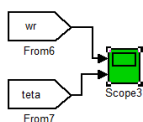
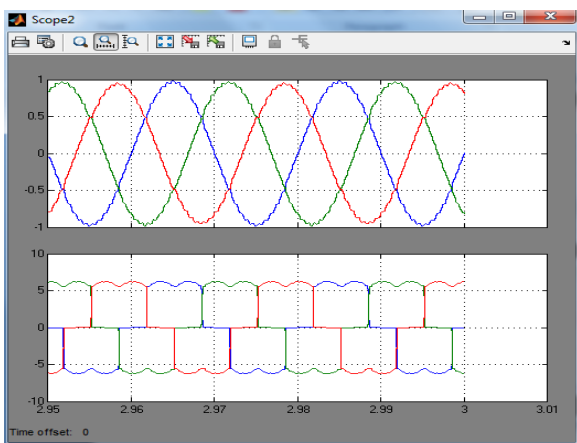
GSC and RSC side converters



Field excitation system of DFIG

Outputs:





REFERENCES

- [1] W. Qiao and R. G. Harley, "Grid connection requirements and solutions for DFIG wind turbines," in Proc. IEEE Energy 2030 Conf. (ENERGY'08), Nov. 17–18, 2008, pp. 1–8.
- [2] S. Muller, M. Deicke, and R. W. De Doncker, "Doubly fed induction generator systems for wind turbines," IEEE Ind. Appl. Mag., vol. 8, no. 3, pp. 26–33, May/Jun. 2002.
- [3] I. Munteanu, A. I. Bratcu, N.-A. Cutululis, and E. Ceang, Optimal Control of Wind Energy Systems Towards a Global Approach. Berlin, Germany: Springer-Verlag, 2008.
- [4] A. A. B. MohdZin, H. A. Mahmoud Pesaran, A. B. Khairuddin, L. Jahanshaloo, and O. Shariati, "An overview on doubly fed induction generators controls and contributions to wind based electricity



generation,” *Renew. Sustain. Energy Rev.*, vol. 27, pp. 692–708, Nov. 2013.

[5] S. S. Murthy, B. Singh, P. K. Goel, and S. K. Tiwari, “A comparative study of fixed speed and variable speed wind energy conversion systems feeding the grid,” in *Proc. IEEE Conf. Power Electron. Drive Syst. (PEDS’07)*, Nov. 27–30, 2007, pp. 736–743.

[6] D. S. Zinger and E. Muljadi, “Annualized wind energy improvement using variable speeds,” *IEEE Trans. Ind. Appl.*, vol. 33, no. 6, pp. 1444–1447, Nov./Dec. 1997.

[7] H. Polinder, F. F. A. van der Pijl, G. J. de Vilder, and P. J. Tavner, “Comparison of direct-drive and geared generator concepts for wind turbines,” *IEEE Trans. Energy Convers.*, vol. 21, no. 3, pp. 725–733, Sep. 2006.

[8] R. Datta and V. T. Ranganathan, “Variable-speed wind power generation using doubly fed wound rotor induction machine—A comparison with alternative schemes,” *IEEE Trans. Energy Convers.*, vol. 17, no. 3, pp. 414–421, Sep. 2002.

[9] E. Muljadi, C. P. Butterfield, B. Parsons, and A. Ellis, “Effect of variable speed wind turbine generator on stability of a weak grid,” *IEEE Trans. Energy Convers.*, vol. 22, no. 1, pp. 29–36, Mar. 2007.